Available online at www.sciencedirect.com

ScienceDirect

Current Opinion in Cell Biology

Molecular architecture of the actin cytoskeleton: From single cells to whole organisms using cryo-electron tomography

Jonathan Schneider[1,2] and Marion Jasnin[2,3]

Abstract

Cryo-electron tomography (cryo-ET) has begun to provide intricate views of cellular architecture at unprecedented resolutions. Considerable efforts are being made to further optimize and automate the cryo-ET workflow, from sample preparation to data acquisition and analysis, to enable visual proteomics inside of cells. Here, we will discuss the latest advances in cryo-ET that go hand in hand with their application to the actin cytoskeleton. The development of deep learning tools for automated annotation of tomographic reconstructions and the serial lift-out sample preparation procedure will soon make it possible to perform high-resolution structural biology in a whole new range of samples, from multicellular organisms to organoids and tissues.

Addresses

[1] Department of Molecular Structural Biology, Max Planck Institute of Biochemistry, 82152 Martinsried, Germany

[2] Helmholtz Pioneer Campus, Helmholtz Munich, 85764 Neuherberg, Germany

[3] Department of Chemistry, Technical University of Munich, 85748 Garching, Germany

Corresponding author: Jasnin, Marion (marion.jasnin@helmholtz-munich.de)

Current Opinion in Cell Biology 2024, **88**:102356

This review comes from a themed issue on **Cell Architecture 2024**

Edited by **Ohad Medalia** and **Carsten Janke**

For complete overview of the section, please refer the article collection - Cell Architecture 2024

Available online 11 April 2024

https://doi.org/10.1016/j.ceb.2024.102356

Keywords

Cryo-electron tomography, Molecular sociology, Actin filaments, Tomogram acquisition, Automation, Deep learning-based data analysis, Lift-out.

Introduction

Over the last decade, cryo-electron microscopy (cryo-EM), in particular single-particle analysis (SPA), has become a key technique for studying the structure of macromolecular complexes. It has proved indispensable in the field of the actin cytoskeleton, where it was used to reconstruct the three-dimensional (3D) structure of the actin filament at high resolution [1]. Since then, a plethora of structures have been determined, elucidating the interactions between actin and various actin-binding proteins [2–5], actin isoforms [6], the mechanisms of filament aging and phosphate release [7–9], and structural alterations during filament bending [10]. In addition, the cryo-EM structures of the human cardiac thin and thick filaments have been both resolved [11,12].

Traditional structural biology methods, including SPA, work mainly on isolated samples and purified macromolecules. However, molecular complexes often only fold and assemble correctly in the right cellular environment. Moreover, biological functions and pathways are rarely the result of a single macromolecule. The interplay between several biological components, and their correct positioning and spatial arrangement within the cell, is essential for many cellular processes. This concept has been called the "molecular sociology of the cell" [13]. Cryo-electron tomography (cryo-ET) enables macromolecular complexes to be studied directly within their native functional environment with sub-nanometer resolution [14]. The spatial arrangement and interactions of the cellular components involved can be uncovered and deciphered.

With the exception of very small, thin bacterial cells and the cell periphery, the cell interior is too thick for direct imaging with a transmission electron microscope. Therefore, after vitrification by plunge freezing, cells are thinned to electron transparency (typically 100–300 nm) using cryo-focused ion beam (cryo-FIB) milling, where the material above and below the region of interest is ablated [15] (Figure 1a). The remaining cellular section is called a lamella. Large biological samples, such as large cells (typically >10 µm thick), multicellular organisms or tissues, require vitrification by high-pressure freezing and sample extraction using the cryo-lift-out technique [16], which will be discussed later in this review (Figure 1b).

For cryo-ET imaging, two-dimensional projection images are generated at different tilt angles, known as

Figure 1

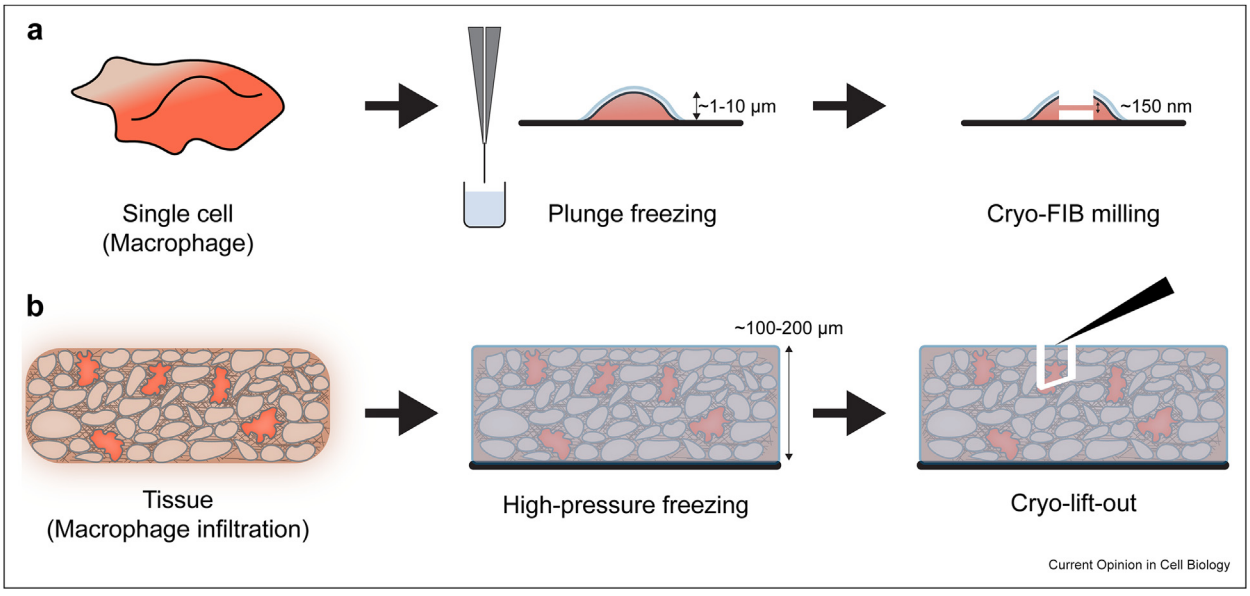

Sample preparation workflow for cryo-ET exploration. a. Sample preparation workflow for single cells, such as human macrophages, or unicellular organisms. Adherent cells or cell clumps are vitrified by plunge-freezing in liquid ethane. This vitrification method is applicable for cells less than 10 µm thick. The sample is then thinned to electron transparency (<500 µm, typically 100–300 nm) using cryo-FIB milling. **b.** Large cells, multicellular organisms or tissues (for example during macrophage infiltration) are vitrified by high-pressure freezing. The typical thickness of an HPF sample is between 100 and 200 µm, depending on the spacers used. A sample block is then extracted by cryo-lift-out and thinned to electron transparency using cryo-FIB milling.

tilt series. This set of projection images can then be computationally combined into a 3D volume, called a tomogram, which contains high-resolution structural information. Tomograms with several copies of a macromolecule of interest are suitable for subtomogram averaging (STA). As with SPA, multiple sub-volumes comprising the structure of interest are extracted and computationally combined to generate a volume with a significantly improved signal-to-noise ratio and higher resolution. For a detailed description of cryo-ET in general and STA in particular, the reader is invited to read several excellent reviews [14,15,17]. Below, we present the latest advances in cryo-ET and how they have enabled structural exploration of the cytoskeleton at molecular resolution, both in single cells and in whole organisms, with a particular focus on actin.

Muscle sarcomeres, an ideal system for cryo-ET imaging

Cryo-ET, combined with STA, is perfectly suited to the study of the cytoskeleton. The actin cytoskeleton provided the first examples of the power of cryo-ET to explore cell architecture [18,19]. Over the last years, numerous studies have exploited cryo-ET, for example to reveal the mechanism of propagation of actin waves [20], the embedding of stress fibers in a contractile cortical network [21], the interface between actin filaments and integrins in platelet pseudopodia [22], the mechanism of force generation by macrophage podosomes [23], the modulation and remodeling of actin filaments in neuronal growth cones and axon branches [24–26], the role of different Arp2/3 complex isoforms in lamellipodia architecture [27], the structural basis of sarcomere contractility [28–32], and actin remodeling during glucose-induced insulin secretion in beta cells [33]. Cryo-ET has also been used for exploratory purposes, for example to show the presence of actin filaments within the microtubule lumen [34] or the existence of an actin-based cytoskeleton in Asgard archea [35].

Most of these studies have been carried out in the cytosol of eukaryotic cells, with missing data in yeast, where detection of cytoskeletal features has proved difficult, partly due to the high density of the cytoplasm. Similarly, detection of nuclear actin filaments in mammalian cells poses major challenges, suggesting that filaments may be very short and difficult to detect in the dense nuclear interior. This is currently one of the main limitations in cryo-ET data analysis, where small cellular features are difficult to identify due to the lack of appropriate detection tools. In addition, cryo-ET suffers from the “missing wedge” problem, i.e. incomplete sampling due to the limited tilt range during data acquisition, which also leads to an elongation in z. However, this problem can be solved by collecting tomograms of actin structures in different orientations, as well as using STA to recover missing structural information from the filaments.

Myofibrils have proven to be an ideal sample for cryo-FIB sample preparation and STA due to their geometry and the regular organization of their components. They have been used to provide unique insights into the structure of actin-binding proteins in near-native conditions. For example, the sarcomeric protein nebulin, one of the largest mammalian proteins, could not be resolved either by X-ray crystallography or by SPA due to its very large size, flexible nature and unique interactions with the thin filament. Using cryo-ET and STA, its structure and interaction with the core actin filament were elucidated in myofibrils isolated from mouse skeletal muscle at high resolution [30]. In addition, the structure of the thick filament has recently been resolved in relaxed mouse cardiac myofibrils, revealing in unprecedented detail the interaction between myosin, myosin protein binding C and titin [31]. This pioneering work paves the way for further exploration of the structure of the thick filament in different states of contraction and for an in-depth understanding of sarcomere function and regulation. Finally, a new preprint presented a cryo-ET platform for studying cardiovascular structural biology in human induced pluripotent stem cell-derived cardiomyocytes, which could be useful for studying the impact of cardiomyopathy-associated mutations on protein structure [32]. All these cryo-ET studies have begun to provide a molecular picture of the architecture and interconnectivity of the sarcomeric components that enable contractility. Many important questions remain about the organization of sarcomeres in human cells and tissues, particularly in the context of heart and muscle disease, for which sophisticated sample preparation methods, such as lift-out, are required.

Towards improved data collection and analysis

Cryo-ET in combination with STA provides lower resolution structures than SPA, with good samples reaching below 10 Å and, in ideal cases, down to 4.5 Å for actin and actin-related proteins [30,36,37]. It has been suggested that the main limitation in terms of resolution is the initial alignment of the tilt series, which can be partially corrected using multi-particle refinement [38–40]. It has therefore been argued that the main advantage of SPA over cryo-ET is the much faster data acquisition and the ability to obtain larger datasets. Cryo-ET remains a low throughput method and is more labor intensive than SPA. Considerable efforts are currently being made to speed up tilt series acquisition and tomogram annotation.

Automation of data acquisition

Acquiring a tilt series takes much longer than acquiring a single projection image. The stage must be tilted and stabilized, and the area of interest recentered and focused before an image can be acquired. This is why most tomographic data acquisition software now uses multishot acquisition, where several tilt series are recorded in parallel using the beam-image shift, while using a single tilt series for tracking and focusing [41,42] (Figure 2a–b).

The open-source PACE-tomo (parallel automated cryo-electron tomography) software uses a geometrical model of the sample to predict the motion for each position across the lamella, enabling tens of tilt series to be acquired at a time and reducing acquisition time to ~5 min per position [36]. The authors reconstructed the structure of the actin filament in complex with tropomyosin in mouse mammary gland epithelial cells at a resolution of 12 Å. This structure was generated from 4 of 7 tilt series, which were acquired in just 30 min, highlighting the importance of rapid acquisition to optimize the imaging area covered and quickly assess the sample quality. This can be done all the more easily thanks to current developments in on-the-fly pre-processing and analysis of tilt series [43,44].

Whereas for homogeneous samples in SPA, acquisition areas are selected automatically on the basis of ice thickness, cryo-ET still requires user intervention for target selection. On-the-fly pre-processing of the tilt series already helps to assess whether a target of interest is present in the selected area of the lamella. PACE-tomo's capabilities have also recently been enhanced by the use of machine learning to facilitate target selection. SPACE-tomo (smart parallel automated cryo-electron tomography) enables automated detection of lamellae and classification of their quality, segmentation of organelles such as mitochondria and automated selection of suitable acquisition areas [45].

Another exciting development is the introduction of square beams for montage tomography, using a dedicated C2 aperture that is applicable to modern TEM instruments [46]. In montage tomography, multiple image tiles are acquired with some overlap and then stitched together to obtain a large tomogram, thus combining high magnification and a larger field of view [47,48]. Square-beam imaging reduces the overlap required between adjacent tiles, and limits the areas that are illuminated but not captured by the detector. This results in a more efficient and evenly distributed electron dose.

Deep learning-based data analysis

With rapid advances in automated data acquisition, efficient workflows for data analysis are becoming increasingly essential. Tilt series can be processed and tomograms reconstructed automatically using various software solutions [44,49–53]. However, tomogram annotation is time consuming and current efforts in deep learning aim to improve this limitation. In the last two years, a few tools have been published that use deep

Figure 2

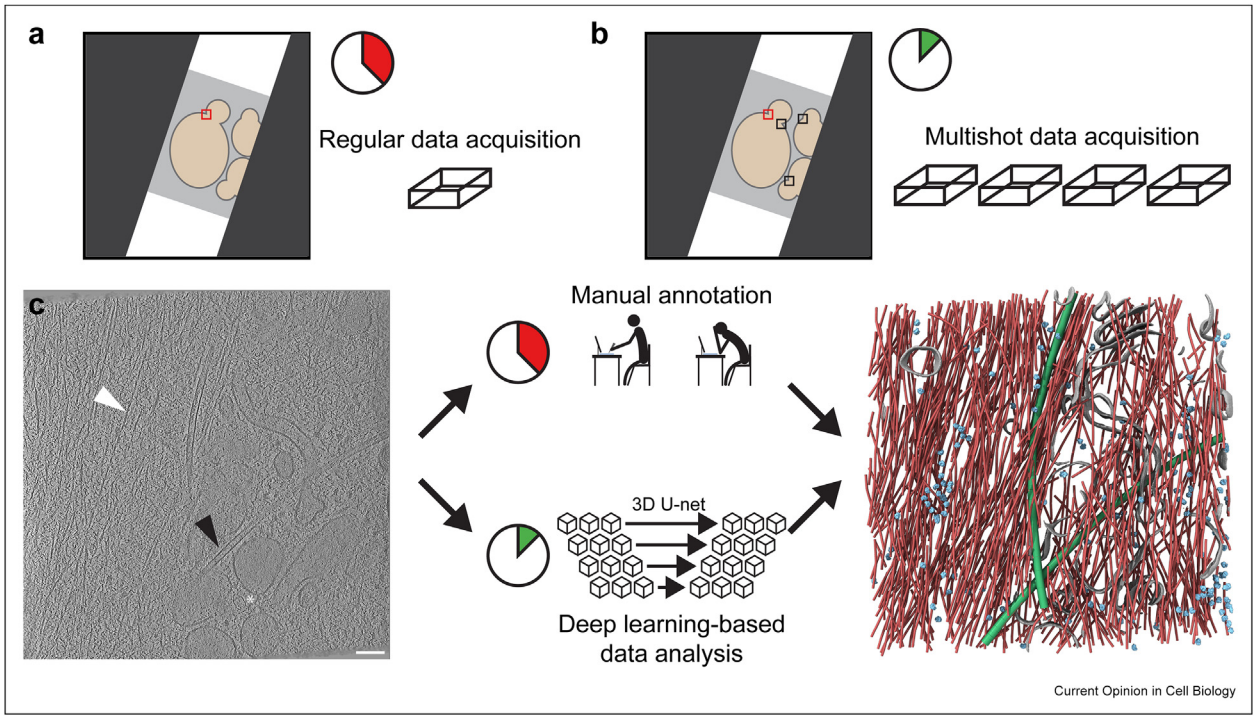

Improved data collection and analysis. a. Acquisition of a single tilt series. The red target area contains a region of interest, tracking and focusing during acquisition is usually performed in a different area along the tilt-axis of the microscope. **b.** Improved tilt series acquisition using multishot tomography, as implemented in PACE-tomo [36]. The red target area is the tracking tilt series. The additional acquisition areas in black are acquired simultaneously. When the stage is tilted, the sample geometry is taken into account to image the correct targets. This reduces the acquisition time for a single tomogram to less than 10 min. **c.** Annotation of a tomogram. Left: Tomographic slice of the basal membrane of a vitrified primary human macrophage exposed after cryo-FIB sample preparation. An actin filament and a microtubule are indicated by a white and black arrow, respectively. The asterisk indicates the Vault protein. Scale bar: 100 nm. Middle: Manual segmentation of membranes and filaments is time-consuming. Recent deep learning tools based on 3D U-nets considerably speed up tomogram annotation. Right: Segmentation of the tomogram shown on the left. Actin filaments are shown in red, microtubules in green, ribosomes in light blue and membranes in gray.

learning algorithms and pre-trained models or training datasets to locate and identify various cellular components (Figure 2c). We will cover here not only the tools developed for the detection of actin filaments, but also for organelles, membranes and macromolecules, as understanding actin functions in cells requires the ability to detect all its interaction partners, for example to quantify distances separating them or the sites of interaction.

The MemBrain deep learning software automatically and reliably segments membranes from tomograms and can also automatically detect membrane-bound proteins [54,55]. Moreover, it does not require extensive manual corrections, as is usually the case with semi-automated segmentation tools [56,57]. Complementary software solutions are used to locate and identify macromolecules in tomographic volumes. DeePiCt (deep picker in context) is based on convolutional neural networks (CNNs) and enables supervised detection of macromolecular complexes in the cellular environment [58]. DeePiCt has been trained on fully annotated yeast tomograms and has been successfully applied to the structural exploration of distinct ribosome subpopulations. It has also been used to detect cytoskeletal components, in particular microtubules and actin filaments, although actin segmentation would benefit from more training data and sampling of different orientations to improve performance. TomoTwin is another generalized particle picking model based on deep metric learning, which enables *de novo* identification of macromolecules in tomograms [59]. It does not require user-generated training data and is therefore less user-biased. Its applicability to the detection of cytoskeletal filaments would require optimization of the underlying models.

Commercial Dragonfly software has been used to generate tomogram segmentations based on multi-slice U-Net CNNs, where multiple target structures are segmented simultaneously [60]. The approach has been used to automatically segment actin filaments. In

addition, based on training on synthetic data, the authors were able to differentiate bare actin filaments from cofilin-decorated actin filaments [61]. Such synthetic datasets can serve as ground truth for new deep learning approaches and make time-consuming manual annotations redundant [62].

All these developments represent a promising step towards the identification and annotation of cellular features in tomograms, but considerable efforts are still needed to be able to extract all the information present. The development of foundation models for cryo-ET data would be a major step forward, but would require access to a broad spectrum of generalized data, which is currently lacking.

Towards exploring larger samples

The ability to explore large cells, multicellular organisms, organoids or tissues is the latest advance in cryo-ET. Cryo-FIB milling is generally limited to cell samples that are thin enough to be vitrified by plunge freezing (Figure 1a). Unexpectedly, human oocytes, the largest mammalian cells, have been successfully sectioned by cryo-FIB milling, with an additional orthogonal milling step [63]. However, this approach relies on the use of large quantities of cryo-protectant [64], the effects of which on the structural integrity of the cell at the molecular level, in particular the cytoskeleton, remains to be studied.

Large biological samples must be high pressure frozen (HPF) in order to achieve vitrification. A procedure called lift-out is then required to extract the samples from the thick layer of ice in which they are embedded, so that lamellae can be prepared (Figure 1b). Cryo-lift-out uses a micromanipulator in the form of a needle tip or gripper to extract a small volume and place it on a receiver grid where the sample is reattached and then thinned using cryo-FIB milling [16,65]. A new study has developed a platform to grow human foreskin fibroblast extracellular matrix (ECM) on EM grids and explore the structural landscape of the ECM using lift-out and cryo-ET [66]. This made it possible to visualize a network of ECM fibers, such as collagen and unknown fibrillar structures, as well as their relative positioning with respect to the surrounding cells. This is particularly interesting because of the coupling between the actin cytoskeleton and the ECM via the adhesion machinery as exemplified during macrophage migration, matrix degradation or cell invasion [22,23].

Sampling whole organisms with serial lift-out

Cryo-lift-out is a time-consuming and labor-intensive technique, and the success rate is generally low. As a result, it is not yet widely used. Thanks to a new lift-out procedure, known as serial lift-out (SLO), it is now possible to extract sections in series from a single lift-out transfer, significantly increasing yield [67] (Figure 3a). A similar approach has been described and called SOLIST (serialized on-grid lift-in sectioning for tomography) [68]. SLO was performed on *Caenorhabditis elegans* (*C. elegans*) L1 larvae, where the whole worm was extracted from an HPF waffle grid (Figure 3b). Waffle samples are vitrified by high-pressure freezing on an EM grid sandwiched between two HPF carriers [69]. This reduces the thickness of the HPF sample to the height of the grid, greatly reducing the milling time required to extract a block of sample. In the study, the extracted bulk sample containing a *C. elegans* larva was sequentially sliced into transversal sections approximately 1–2 µm thick, each of which was then thinned to the thickness of a typical lamella. In this way, multiple consecutive lamellae were generated transverse to the main axis of the worm, revealing the molecular anatomy of the worm over its entire height.

The authors captured the body wall muscle, a cell type prominent in transverse sections, allowing direct visualization of the hexagonal packing and interconnection of thin and thick filaments (Figure 3c–d), previously observed only in longitudinal sections [28–32]. In addition, the authors highlighted the singular structure of microtubules in *C. elegans*, which is mainly composed of 11 protofilaments (pfs), except in touch receptor cells, which typically contain 15 pf microtubules. In a single tomogram, the authors show both types of microtubules located in adjacent cells, highlighting the importance of imaging biological structures in their native cellular context (Figure 3e–h). They also resolved several translational states of the ribosome (Figure 3h).

Future perspectives

Now that the cryo-ET workflow is well established and more and more cell biologists have begun to exploit this powerful approach for their studies, the range of actin systems that could be explored is likely to expand rapidly. For example, we could imagine cryo-ET work on actin-spectrin scaffolds in neurons, which would bring valuable complementary information to existing platinum-replica studies. In addition, the development of deep-learning tools for the detection of short or crosslinked filament networks, particularly in noisy tomograms, will make elusive actin structures such as nuclear actin filaments or actin filaments in yeast accessible. Cofilin-actin rods are already detectable by cryo-ET and will probably be the first nuclear actin structures to be characterized.

The serial lift-out method makes it possible to examine a whole new range of complex biological samples, such as multicellular organisms, organoids or tissues, at higher throughput. This paves the way for exciting research experiments, particularly in the field of the actin cytoskeleton. Here again, myofibrils would be a prime

Figure 3

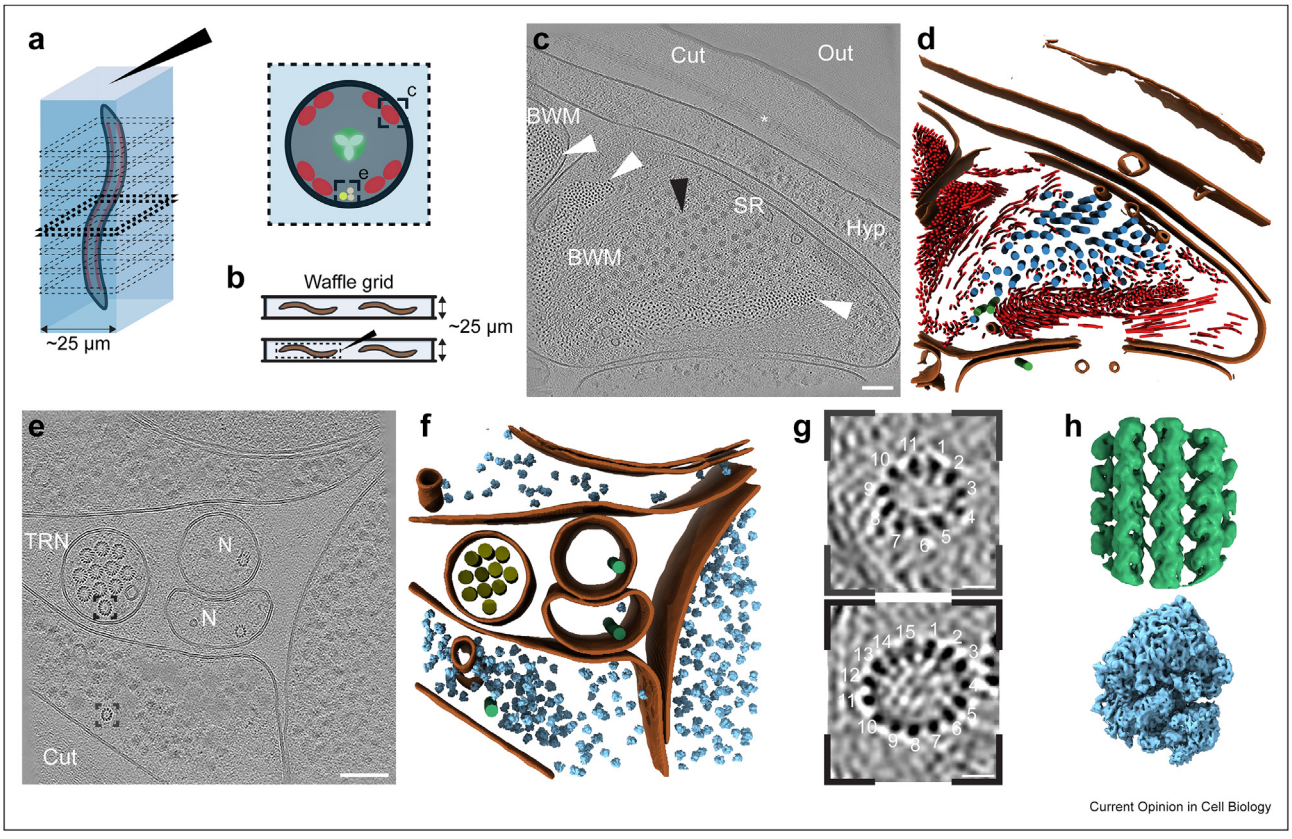

Sampling the molecular anatomy of a *C. elegans* larva using serial lift-out and cryo-ET. a. Schematic illustration of the serial lift-out method applied to a *C. elegans* L1 larva [67]. Serial sections are prepared from one lift-out volume containing a single larva. One slice highlighted on the left is shown as a schematic top view on the right, with the black boxes indicating the areas imaged in **c** and **e**. **b.** Schematic view of an HPF sample prepared using the waffle method [69]. **c.** Tomographic slice of body wall muscle (BWM, EMD-17246). Bundles of thin filaments are shown by white arrows, a thick filament is indicated by a black arrow. SR: sarcoplasmic reticulum. The main BWM is surrounded by a second BWM, both bordered by a hypodermal cell (Hyp), followed by a layer of collagen (indicated by an asterisk) within the cuticle (Cut). **d.** Segmentation of the tomogram shown in **c**. Thin filaments are shown in red, thick filaments in blue, microtubules in green and membranes in brown. **e.** Tomographic slice of a presumed part of the ventral sublateral nerve cord (EMD-18186), including a touch receptor neuron (TRN) and other putative neurons (N). The TRN is characterized by a microtubule array of 15 pfs, compared with 11 pfs in other cells. **f.** Corresponding segmentation. The 11 pf microtubules are colored in green, the 15 pf microtubules in green–brown, ribosomes are shown in light blue and membranes in brown. **g.** Close-up view of the regions boxed in **e**, showing an 11 pf microtubule (gray, top) and a 15 pf microtubule (black, bottom), respectively. **h.** Top: Subtomogram average of a subsection of the 11 pf microtubule, resolved at 13 Å (EMD-18187). Bottom: Subtomogram average of a ribosome at 6.9 Å resolution (EMD-17241). **c**, **e**: Scale bars: 100 nm. **g**: Scale bars: 10 nm.

sample for serial lift-out: waffle samples of skeletal or cardiac myofibrils could be easily prepared to visualize the molecular architecture of serially arranged sarcomeres in transverse or oblique sections. Cell migration and invasion could also be studied directly in a 3D tissue environment to generate molecular views along the migratory pathway throughout the tissue. Cryo-ET of lift-out samples would provide valuable structural information on adhesion complexes and transmembrane proteins, which could be captured in multiple orientations rather than in the single plane of the carbon film of an EM grid. We believe that these experiments will be feasible over the next few years and will provide exciting insights into these essential biological processes.

Funding

The work was funded by the Deutsche Forschungsgemeinschaft (DFG) call ANR-DFG 2020 NLE for the project no. JA-3038/2-1 (to MJ).

Author contribution

All authors contributed to the conceptualization and writing of the manuscript.

Declaration of competing interest

The authors declare that they have no known competing financial interests or personal relationships that could

have appeared to influence the work reported in this paper.

Data availability

No data was used for the research described in the article.

References

Papers of particular interest, published within the period of review, have been highlighted as:

- • of special interest
- •• of outstanding interest

1. Galkin VE, Orlova A, Vos MR, Schroder GF, Egelman EH: **Near-atomic resolution for one state of F-actin**. *Structure* 2015, **23**: 173–182.
2. Mei L, Espinosa de Los Reyes S, Reynolds MJ, Leicher R, Liu S, Alushin GM: **Molecular mechanism for direct actin force-sensing by alpha-catenin**. *eLife* 2020, **9**:e62514.
3. Mei L, Reynolds MJ, Garbett D, Gong R, Meyer T, Alushin GM: **Structural mechanism for bidirectional actin cross-linking by T-plastin**. *Proc Natl Acad Sci U S A* 2022, **119**:e2205370119.
4. Ding B, Narvaez-Ortiz HY, Singh Y, Hocky GM, Chowdhury S, Nolen BJ: **Structure of Arp2/3 complex at a branched actin filament junction resolved by single-particle cryo-electron microscopy**. *Proc Natl Acad Sci U S A* 2022, **119**:e2202723119.
5. Gong R, Reynolds MJ, Hamilton K, Alushin GM: **Fascin structural plasticity mediates flexible actin bundle construction**. *bioRxiv* 2024. 2024.01.03.574123.
6. Arora AS, Huang HL, Singh R, Narui Y, Suchenko A, Hatano T, Heissler SM, Balasubramanian MK, Chinthalapudi K: **Structural insights into actin isoforms**. *eLife* 2023, **12**:e82015.
7. Oosterheert W, Klink BU, Belyy A, Pospich S, Raunser S: **Structural basis of actin filament assembly and aging**. *Nature* 2022, **611**:374–379.
8. Oosterheert W, Blanc FEC, Roy A, Belyy A, Sanders MB, Hofnagel O, Hummer G, Bieling P, Raunser S: **Molecular mechanisms of inorganic-phosphate release from the core and barbed end of actin filaments**. *Nat Struct Mol Biol* 2023, **30**: 1774–1785.
9. Chou SZ, Pollard TD: **Cryo-EM structures of both ends of the actin filament explain why the barbed end elongates faster than the pointed end**. *bioRxiv* 2023. 2023.05.12.540494.
10. Reynolds MJ, Hachicho C, Carl AG, Gong R, Alushin GM: **Bending forces and nucleotide state jointly regulate F-actin structure**. *Nature* 2022, **611**:380–386.
11. Yamada Y, Namba K, Fujii T: **Cardiac muscle thin filament structures reveal calcium regulatory mechanism**. *Nat Commun* 2020, **11**:153.
12. Dutta D, Nguyen V, Campbell KS, Padron R, Craig R: **Cryo-EM structure of the human cardiac myosin filament**. *Nature* 2023, **623**:853–862.
13. Beck M, Baumeister W: **Cryo-electron tomography: can it reveal the molecular sociology of cells in atomic detail?** *Trends Cell Biol* 2016, **26**:825–837.
14. Turk M, Baumeister W: **The promise and the challenges of cryo-electron tomography**. *FEBS Lett* 2020, **594**:3243–3261.
15. Young LN, Villa E: **Bringing structure to cell biology with cryo-electron tomography**. *Annu Rev Biophys* 2023, **52**:573–595.
16. Kuba J, Mitchels J, Hovorka M, Erdmann P, Berka L, Kirmse R, J KO, J DEB, Goetze B, Rigort A: **Advanced cryo-tomography workflow developments – correlative microscopy, milling automation and cryo-lift-out**. *J Microsc* 2021, **281**:112–124.
17. Wan W, Briggs JA: **Cryo-electron tomography and subtomogram averaging**. *Methods Enzymol* 2016, **579**:329–367.
18. Medalia O, Weber I, Frangakis AS, Nicastro D, Gerisch G, Baumeister W: **Macromolecular architecture in eukaryotic cells visualized by cryoelectron tomography**. *Science* 2002, **298**:1209–1213.
19. Medalia O, Beck M, Ecke M, Weber I, Neujahr R, Baumeister W, Gerisch G: **Organization of actin networks in intact filopodia**. *Curr Biol* 2007, **17**:79–84.
20. Jasnin M, Beck F, Ecke M, Fukuda Y, Martinez-Sanchez A, Baumeister W, Gerisch G: **The architecture of traveling actin waves revealed by cryo-electron tomography**. *Structure* 2019: 1211–1223.e5.
21. Vignaud T, Copos C, Leterrier C, Toro-Nahuelpan M, Tseng Q, Mahamid J, Blanchoin L, Mogilner A, Thery M, Kurzawa L: **Stress fibres are embedded in a contractile cortical network**. *Nat Mater* 2021, **20**:410–420.
22. Sorrentino S, Conesa JJ, Cuervo A, Melero R, Martins B, Fernandez-Gimenez E, de Isidro-Gomez FP, de la Morena J, Studt JD, Sorzano COS, *et al.*: **Structural analysis of receptors and actin polarity in platelet protrusions**. *Proc Natl Acad Sci U S A* 2021, **118**:e2105004118.
23. Jasnin M, Hervy J, Balor S, Bouissou A, Proag A, Voituriez R, Schneider J, Mangeat T, Maridonneau-Parini I, Baumeister W, *et al.*: **Elasticity of podosome actin networks produces nanonewton protrusive forces**. *Nat Commun* 2022, **13**:3842.
24. Atherton J, Stouffer M, Francis F, Moores CA: **Visualising the cytoskeletal machinery in neuronal growth cones using cryo-electron tomography**. *J Cell Sci* 2022, **135**:jcs259234.
25. Hylton RK, Heebner JE, Grillo MA, Swulius MT: **Cofilactin filaments regulate filopodial structure and dynamics in neuronal growth cones**. *Nat Commun* 2022, **13**:2439.
26. Nedozralova H, Basnet N, Ibiricu I, Bodakuntla S, Biertumpfel C, Mizuno N: **In situ cryo-electron tomography reveals local cellular machineries for axon branch development**. *J Cell Biol* 2022, **221**:e202106086.
27. Fassler F, Javoor MG, Datler J, Doring H, Hofer FW, Dimchev G, Hodirnau VV, Faix J, Rottner K, Schur FKM: **ArpC5 isoforms regulate Arp2/3 complex-dependent protrusion through differential Ena/VASP positioning**. *Sci Adv* 2023, **9**:eadd6495.
28. Burbaum L, Schneider J, Scholze S, Bottcher RT, Baumeister W, Schwille P, Plitzko JM, Jasnin M: **Molecular-scale visualization of sarcomere contraction within native cardiomyocytes**. *Nat Commun* 2021, **12**:4086.
29. Wang Z, Grange M, Wagner T, Kho AL, Gautel M, Raunser S: **The molecular basis for sarcomere organization in vertebrate skeletal muscle**. *Cell* 2021, **184**:2135–2150.e13.
30. •• Wang Z, Grange M, Pospich S, Wagner T, Kho AL, Gautel M, Raunser S: **Structures from intact myofibrils reveal mechanism of thin filament regulation through nebulin**. *Science* 2022, **375**:eabn1934.

This work presents the in situ structure of the sarcomeric protein nebulin, one of the largest mammalian proteins. Due to its large size, flexible nature and unique interaction with the thin filament, its structure could not be obtained by X-ray crystallography or cryo-EM SPA.

31. • Tamborrini D, Wang Z, Wagner T, Tacke S, Stabrin M, Grange M, Kho AL, Rees M, Bennett P, Gautel M, *et al.*: **Structure of the native myosin filament in the relaxed cardiac sarcomere**. *Nature* 2023, **623**:863–871.

The authors revealed the structure of the thick filament in relaxed cardiac myofibrils using cryo-ET, which was not previously possible due to its complexity.

32. Woldeyes RA, Nishiga M, Vander Roest AS, Engel L, Giri P, Montenegro GC, Wu AC, Dunn AR, Spudich JA, Bernstein D, *et al.*: **Cryo-electron tomography reveals the structural diversity of cardiac proteins in their cellular context**. *bioRxiv* 2023. 2023.10.26.564098.
33. Li W, Li A, Yu B, Zhang X, Liu X, White KL, Stevens RC, Baumeister W, Sali A, Jasnin M, *et al.*: **In situ structure of actin**

remodeling during glucose-stimulated insulin secretion using cryo-electron tomography. *Nat Commun* 2024, **15**:1311.

34. Paul DM, Mantell J, Borucu U, Coombs J, Surridge KJ, Squire JM, Verkade P, Dodding MP: **In situ cryo-electron tomography reveals filamentous actin within the microtubule lumen**. *J Cell Biol* 2020, **219**:e201911154.

35. Rodrigues-Oliveira T, Wollweber F, Ponce-Toledo RI, Xu J, Rittmann SKR, Klingl A, Pilhofer M, Schleper C: **Actin cytoskeleton and complex cell architecture in an Asgard archaeon**. *Nature* 2023, **613**:332–339.

36. •• Eisenstein F, Yanagisawa H, Kashihara H, Kikkawa M, Tsukita S, Danev R: **Parallel cryo electron tomography on in situ lamellae**. *Nat Methods* 2023, **20**:131–138.
The authors present an open-source software for the parallel acquisition of several tomograms at the same time. The software determines a geometric model of the sample and uses beam-image shifts to acquire several tilt series simultaneously. This reduces the acquisition time of a tilt series to less than 10 min.

37. Fassler F, Dimchev G, Hodirnau VV, Wan W, Schur FKM: **Cryo-electron tomography structure of Arp2/3 complex in cells reveals new insights into the branch junction**. *Nat Commun* 2020, **11**:6437.

38. Himes BA, Zhang P: **emClarity: software for high-resolution cryo-electron tomography and subtomogram averaging**. *Nat Methods* 2018, **15**:955–961.

39. Tegunov D, Xue L, Dienemann C, Cramer P, Mahamid J: **Multi-particle cryo-EM refinement with M visualizes ribosome-antibiotic complex at 3.5 A in cells**. *Nat Methods* 2021, **18**:186–193.

40. Zivanov J, Oton J, Ke Z, von Kugelgen A, Pyle E, Qu K, Morado D, Castano-Diez D, Zanetti G, Bharat TAM, *et al.*: **A Bayesian approach to single-particle electron cryo-tomography in RELION-4.0**. *eLife* 2022, **11**:e83724.

41. Khavnekar S, Wan W, Majumder P, Wietrzynski W, Erdmann PS, Plitzko JM: **Multishot tomography for high-resolution in situ subtomogram averaging**. *J Struct Biol* 2023, **215**:107911.

42. Bouvette J, Liu HF, Du X, Zhou Y, Sikkema AP, da Fonseca Rezende EMJ, Klemm BP, Huang R, Schaaper RM, Borgnia MJ, *et al.*: **Beam image-shift accelerated data acquisition for near-atomic resolution single-particle cryo-electron tomography**. *Nat Commun* 2021, **12**:1957.

43. Liu HF, Zhou Y, Huang Q, Piland J, Jin W, Mandel J, Du X, Martin J, Bartesaghi A: **nextPYP: a comprehensive and scalable platform for characterizing protein variability in situ using single-particle cryo-electron tomography**. *Nat Methods* 2023, **20**:1909–1919.

44. Tegunov D, Cramer P: **Real-time cryo-electron microscopy data preprocessing with Warp**. *Nat Methods* 2019, **16**:1146–1152.

45. Eisenstein F, Fukuda Y, Danev R: **Smart parallel automated cryo electron tomography**. *bioRxiv* 2023. 2023.12.14.571776.

46. Chua EYD, Alink LM, Kopylov M, Johnston JD, Eisenstein F, de Marco A: **Square beams for optimal tiling in transmission electron microscopy**. *Nat Methods* 2024. https://www.nature.com/articles/s41592-023-02161-x#citeas.

47. Peck A, Carter SD, Mai H, Chen S, Burt A, Jensen GJ: **Montage electron tomography of vitrified specimens**. *J Struct Biol* 2022, **214**:107860.

48. Yang JE, Larson MR, Sibert BS, Kim JY, Parrell D, Sanchez JC, Pappas V, Kumar A, Cai K, Thompson K, *et al.*: **Correlative montage parallel array cryo-tomography for in situ structural cell biology**. *Nat Methods* 2023, **20**:1537–1543.

49. Mastronarde DN, Held SR: **Automated tilt series alignment and tomographic reconstruction in IMOD**. *J Struct Biol* 2017, **197**:102–113.

50. Castano-Diez D: **The Dynamo package for tomography and subtomogram averaging: components for MATLAB, GPU computing and EC2 Amazon Web Services**. *Acta Crystallogr D Struct Biol* 2017, **73**:478–487.

51. Zheng S, Wolff G, Greenan G, Chen Z, Faas FGA, Barcena M, Koster AJ, Cheng Y, Agard DA: **AreTomo: an integrated software package for automated marker-free, motion-corrected cryo-electron tomographic alignment and reconstruction**. *J Struct Biol X* 2022, **6**:100068.

52. Balyschew N, Yushkevich A, Mikirtumov V, Sanchez RM, Sprink T, Kudryashev M: **Streamlined structure determination by cryo-electron tomography and subtomogram averaging using TomoBEAR**. *Nat Commun* 2023, **14**:6543.

53. Khavnekar S, Erdmann P, Wan W: **TOMOMAN: streamlining cryo-electron tomography and subtomogram averaging workflows using TOMOgram MANager**. *Microsc Microanal* 2023, **29**:1020.

54. Lamm L, Righetto RD, Wietrzynski W, Poge M, Martinez-Sanchez A, Peng T, Engel BD: **MemBrain: a deep learning-aided pipeline for detection of membrane proteins in cryo-electron tomograms**. *Comput Methods Programs Biomed* 2022, **224**:106990.

55. • Lamm L, Zufferey S, Righetto RD, Wietrzynski W, Yamauchi KA, Burt A, Liu Y, Zhang H, Martinez-Sanchez A, Ziegler S, *et al.*: **MemBrain v2: an end-to-end tool for the analysis of membranes in cryo-electron tomography**. *bioRxiv* 2024. 2024.01.05.574336.
This work describes a deep learning tool for automatically segmenting membranes in tomograms. It is accompanied by a general model that does not require users to train on their own data and can be used as is.

56. Rigort A, Gunther D, Hegerl R, Baum D, Weber B, Prohaska S, Medalia O, Baumeister W, Hege HC: **Automated segmentation of electron tomograms for a quantitative description of actin filament networks**. *J Struct Biol* 2012, **177**:135–144.

57. Martinez-Sanchez A, Garcia I, Asano S, Lucic V, Fernandez JJ: **Robust membrane detection based on tensor voting for electron tomography**. *J Struct Biol* 2014, **186**:49–61.

58. • de Teresa-Trueba I, Goetz SK, Mattausch A, Stojanovska F, Zimmerli CE, Toro-Nahuelpan M, Cheng DWC, Tollervey F, Pape C, Beck M, *et al.*: **Convolutional networks for supervised mining of molecular patterns within cellular context**. *Nat Methods* 2023, **20**:284–294.
This study presents a deep learning framework for supervised segmentation and template matching in tomographic data. It can be used to detect sparse structures that cannot be identified using traditional template matching tools.

59. Rice G, Wagner T, Stabrin M, Sitsel O, Prumbaum D, Raunser S: **TomoTwin: generalized 3D localization of macromolecules in cryo-electron tomograms with structural data mining**. *Nat Methods* 2023, **20**:871–880.

60. • Heebner JE, Purnell C, Hylton RK, Marsh M, Grillo MA, Swulius MT: **Deep learning-based segmentation of cryo-electron tomograms**. *J Vis Exp* 2022. https://pubmed.ncbi.nlm.nih.gov/36440884/.
This publication provides a workflow for annotating tomographic data using the commercial software Dragonfly, which is becoming increasingly popular in the field.

61. Purnell C, Heebner J, Swulius MT, Hylton R, Kabonick S, Grillo M, Grigoryev S, Heberle F, Waxham MN, Swulius MT: **Rapid synthesis of cryo-ET data for training deep learning models**. *bioRxiv* 2023. 2023.04.28.538636.

62. Martinez-Sanchez A, Lamm L, Jasnin M, Phelippeau H: **Simulating the cellular context in synthetic datasets for cryo-electron tomography**. *bioRxiv* 2023. 2023.05.26.542411.

63. Jentoft IMA, Bauerlein FJB, Welp LM, Cooper BH, Petrovic A, So C, Penir SM, Politi AZ, Horokhovskyi Y, Takala I, *et al.*: **Mammalian oocytes store proteins for the early embryo on cytoplasmic lattices**. *Cell* 2023, **186**:5308–5327.e25.

64. Bäuerlein FJB, Renner M, Chami DE, Lehnart SE, Pastor-Pareja JC, Fernández-Busnadiego R: **Cryo-electron tomography of large biological specimens vitrified by plunge freezing**. *bioRxiv* 2023. 2021.04.14.437159.

65. Schaffer M, Pfeffer S, Mahamid J, Kleindiek S, Laugks T, Albert S, Engel BD, Rummel A, Smith AJ, Baumeister W, *et al.*: **A cryo-FIB**

lift-out technique enables molecular-resolution cryo-ET within native *Caenorhabditis elegans* tissue. *Nat Methods* 2019, **16**:757–762.

66. • Zens B, Fäßler F, Hansen JM, Hauschild R, Datler J, Hodirnau V-V, Zheden V, Alanko J, Sixt M, Schur FK: **Lift-out cryo-FIBSEM and cryo-ET reveal the ultrastructural landscape of extracellular matrix**. *J Cell Biol* 2024, **223**:e202309125.
This work describes a comprehensive workflow for preparing and exploring vitrified sections of the ECM using cryo-lift-out and cryo-ET.

67. •• Schiotz OH, Kaiser CJO, Klumpe S, Morado DR, Poege M, Schneider J, Beck F, Klebl DP, Thompson C, Plitzko JM: **Serial lift-out: sampling the molecular anatomy of whole organisms**. *Nat Methods* 2023. https://pubmed.ncbi.nlm.nih.gov/38110637/.
This study presents a lift-out procedure that makes it possible to prepare multiple serial sections from a single lift-out sample extraction. This method, which is suitable for HPF samples prepared with the waffle method, significantly increases yield.

68. Dung NHT, Perone G, Vazzana R, Don FK, Silva M, Sorrentino S, Swuec P, Leroux F, Kalebic N, Coscia F, *et al.*: **Serialized on-grid lift-in sectioning for tomography (SOLIST)**. *bioRxiv* 2023. 2023.05.11.540146.

69. Kelley K, Raczkowski AM, Klykov O, Jaroenlak P, Bobe D, Kopylov M, Eng ET, Bhabha G, Potter CS, Carragher B, *et al.*: **Waffle method: a general and flexible approach for improving throughput in FIB-milling**. *Nat Commun* 2022, **13**:1857.